

IMPLEMENTATION OF ROUND COLLIDING BEAMS CONCEPT AT VEPP-2000

D. Shwartz^{†1}, D. Berkaev, I. Koop¹, E. Perevedentsev¹, Yu. Rogovsky¹, P. Shatunov, Yu. Shatunov¹, Budker Institute of Nuclear Physics, Novosibirsk, Russia
¹also at Novosibirsk State University, Novosibirsk, Russia

Abstract

VEPP-2000 e^+e^- collider at Budker Institute of Nuclear Physics was commissioned in 2009 and collected data during three runs in whole designed energy range of 160–1000 MeV per beam. The Round Colliding Beams concept was implemented at VEPP-2000 to get a significant enhancement in beam-beam limit. The beam-beam parameter value as high as $\xi = 0.12$ per IP was achieved at intermediate energy. To obtain more intensive beams and achieve target luminosity at top energies the injection chain upgrade was done during 2013–2016. Presently VEPP-2000 is recommissioned and ready to start data taking.

ROUND COLLIDING BEAMS

The VEPP-2000 collider [1] exploits the round beam concept (RBC) [2]. The idea of round-beam collisions was proposed more than 25 years ago for the Novosibirsk Phifactory design [3]. This approach, in addition to the geometrical factor gain, should yield the beam-beam limit enhancement. An axial symmetry of the counter-beam force together with the X – Y symmetry of the transfer matrix between the two IPs provide an additional integral of motion, namely, the longitudinal component of angular momentum $M_z = x'y - xy'$. Although the particles' dynamics remain strongly nonlinear due to beam–beam interaction, it becomes effectively one-dimensional. The reduction of degrees of freedom thins out the resonance grid and suppress the diffusion rate resulting finally in a beam-beam limit enhancement [4].

Thus, there are several demands upon the storage ring lattice suitable for the RBC:

1. Head-on collisions (zero crossing angle).
2. Small and equal β functions at IP ($\beta_x^* = \beta_y^*$).
3. Equal beam emittances ($\varepsilon_x = \varepsilon_y$).
4. Equal fractional parts of betatron tunes ($\nu_x = \nu_y$).

The first three requirements provide the axial symmetry of collisions while requirements (2) and (4) are needed for X – Y symmetry preservation between the IPs.

A series of beam–beam simulations in the weak–strong [5, 6] and strong–strong [7] regimes were done. Simulations showed the achievable values of beam–beam parameters as large as $\xi \sim 0.15$ without any significant blow-up of the beam emittances.

First experimental tests of RBC were carried out at CESR collider with use of linear coupling resonance and specially adopted lattice to fulfil mentioned requirements.

The tests showed promising results of beam-beam parameter increase up to 0.09 but could not provide high luminosity due to large β^* value in this test regime [8].

VEPP-2000 OVERVIEW

The layout of the VEPP-2000 complex as it worked before shutdown for upgrade in 2013 is presented in Fig. 1.

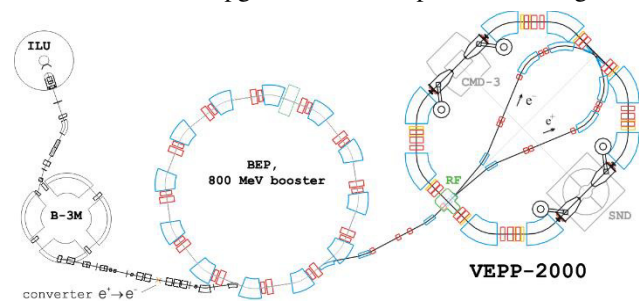


Figure 1: VEPP-2000 complex layout.

VEPP-2000 collider used the injection chain of its predecessor VEPP-2M [9]. It consisted of the old beam production system and Booster of Electrons and Positrons (BEP) with an energy limit of 800 MeV. Collider itself hosts two particle detectors [10], Spherical Neutral Detector (SND) and Cryogenic Magnetic Detector (CMD-3), placed into dispersion-free low-beta straights. The final focusing (FF) is realized using superconducting 13 T solenoids. The main design collider parameters are listed in Table 1. In Fig. 2 one can find a photo of the collider ring.



Figure 2: VEPP-2000 collider photo.

The density of magnet system and detectors components is so high that it is impossible to arrange a beam separation in the arcs. As a result, only a one-by-one bunch collision mode is allowed at VEPP-2000.

[†] d.b.shwartz@inp.nsk.su

Table 1: VEPP-2000 Main Parameters (at $E = 1$ GeV)

Parameter	Value
Circumference, C	24.39 m
Energy range, E	150–1000 MeV
Number of bunches	1×1
Number of particles per bunch, N	1×10^{11}
Betatron functions at IP, $\beta_{x,y}^*$	8.5 cm
Betatron tunes, $\nu_{x,y}$	4.1, 2.1
Beam emittance, $\epsilon_{x,y}$	1.4×10^{-7} m rad
Beam–beam parameters, $\xi_{x,z}$	0.1
Luminosity, L	1×10^{32} cm $^{-2}$ s $^{-1}$

Circular Mode Options

The RBC at VEPP-2000 was implemented by placing two pairs of superconducting focusing solenoids into two interaction regions (IR) symmetrically with respect to collision points. There are several combinations of solenoid polarities that satisfy the round beams' requirements: 'normal round' ($++ \text{---}$), 'Möbius' (M) ($++ \text{--}$) and 'double Möbius' (DM) ($++ \text{++}$) options rotate the betatron oscillation plane by $\pm 90^\circ$ and give alternating horizontal orientation of the normal betatron modes outside the solenoid insertions.

Two 'flat' combinations ($+- \text{--}$ or $+- \text{--}$) are more simple and also satisfy the RBC approach if the betatron tunes lie on the coupling resonance $\nu_x - \nu_y = 2$ to provide equal emittances via X-Y coupling.

All combinations are equivalent in focusing and give the same lattice functions. But the tunes for M and DM options are different due to additional clockwise and counter-clockwise circular mode rotations (see Fig. 3).

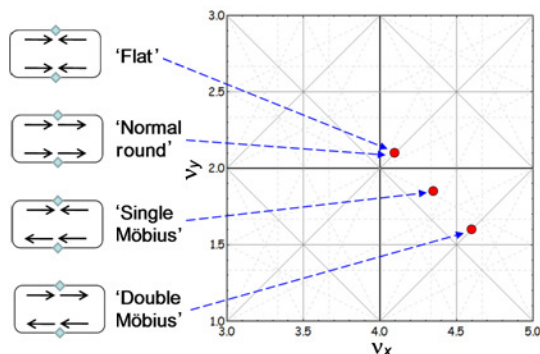


Figure 3: VEPP-2000 round beam options.

Unfortunately, computer simulations showed a serious limitation of the dynamic aperture (DA) for options with mode rotations. A brief experimental study was carried out upon the DM option. At first glance, this case could be preferable, because the tune is a little above 0.5 instead of an integer for the 'flat' mode. However, both the simulation and measurement gave a DA of only $\sim 10 \sigma_{x,y}$. In Fig. 4

the measured DA in terms of beamsize in M-mode is shown as a function of betatron tune.

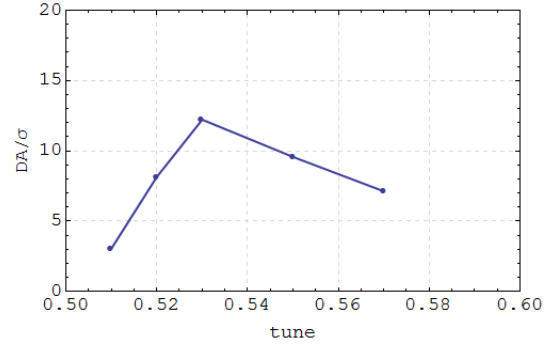


Figure 4: Measured DA in Möbius regime.

The similar problems with DA were reported earlier at CESR collider while trying Möbius regime [11].

Thus hereafter we will suppose conventional 'flat' mode ($+- \text{--}$) with equal emittance due to tunes chosen at the main coupling resonance.

Beam Diagnostics

Beam diagnostics is based on 16 optical CCD cameras that register the visible part of synchrotron light from either end of the bending magnets and give full information about beam positions, intensities, and profiles (see Fig. 5) [12]. In addition to optical beam position monitors (BPM), there are also four electrostatic BPMs in the technical straight sections [13], two photomultipliers for beam current measurements from the synchrotron light intensity, and one beam current transformer as an absolute current monitor.

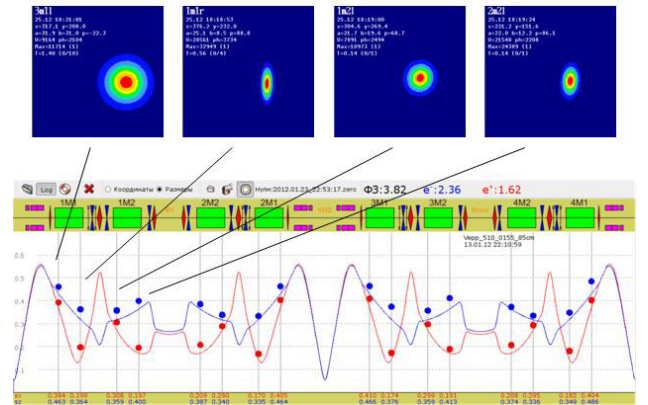


Figure 5: Beam profile measurements.

In addition, VEPP-2000 is equipped with two phi-dissectors – stroboscopic image dissector with electrostatic focusing and deflection. They give information about e^+e^- longitudinal distribution of particles and bunch length [14].

Beam energy is measured online by the Compton backscattering system [15]. In Fig. 6, one can find the typical edge of the spectrum of scattered photons. The oscillations in the left part are produced by interference of the MeV-scale scattered photons due to interaction of electrons with laser radiation along the curved path inside the dipole.

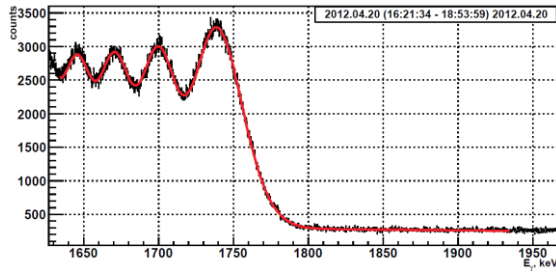


Figure 6: Compton backscattering measurements.

MACHINE TUNING

VEPP-2000 operates in a very wide energy range with strong saturation of magnetic elements at the top energy. For example, the field of conventional iron-dominated bends achieves the value of 2.4 T. In contrast, at low energies the fixed 1.3 T longitudinal field of CMD-3 detector significantly disturbs the focusing. Thus while energy scanning to achieve high luminosity and beam-beam parameter value of great importance is the machine tuning at each energy level. The lattice functions correction is made at VEPP-2000 using Orbit Response Matrix (ORM) analysis [16]. The example of lattice functions before and after correction is presented in Fig. 7.

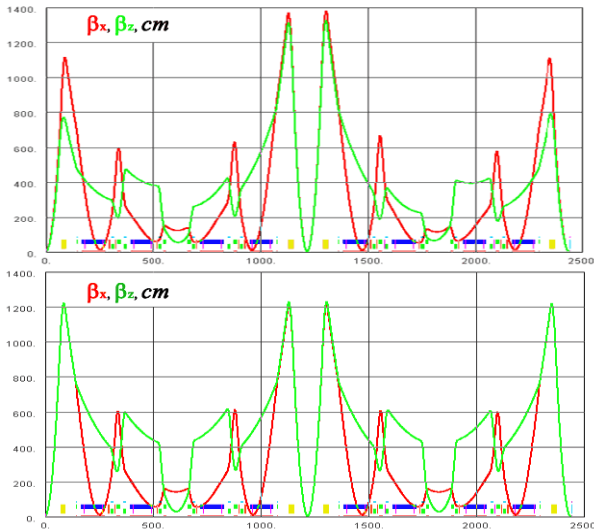


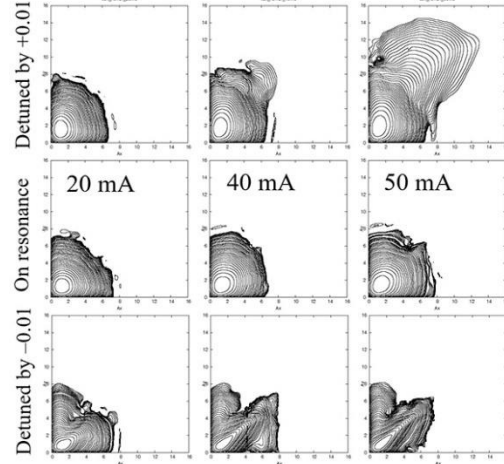
Figure 7: Lattice functions before (up) and after (down) correction.

The ORM is used also to determine and correct closed orbit at quadrupoles by varying their strength, thus using them as additional BPMs. The similar technique is used for final beam-based alignment of solenoids.

Very important it turned out to minimize the dipole correctors' currents, done with help of ORM as well. The reason is poor quality of the steering coils being embedded in quadrupoles due to lack of space.

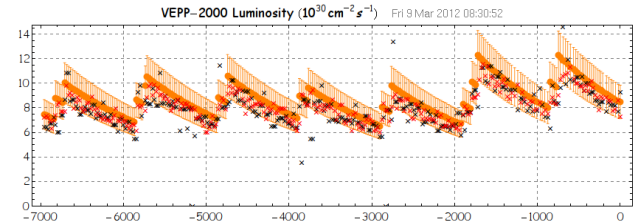
Other parameters need to be tuned carefully are linear coupling in the arcs (tune split < 0.001) [17], and the location of working point (WP) slightly below diagonal of coupling resonance ($\nu_x > \nu_z$). Latter is due to flattening of the beam while shifting from resonance. The tuneshift vector $\{\xi_x, \xi_y\}$ of nonround beam is not parallel with diagonal. If

below diagonal WP self-stabilizes back to resonance, otherwise the shift magnifies itself. In Fig. 8 the results of corresponding *LIFETRAC* [18] simulations are presented. Shown is a transverse beam distribution in terms of normalized amplitudes as a function of counter beam current for three WPs. Beam current of 50 mA corresponds to $\xi \approx 0.11$ at $E = 500$ MeV.

Figure 8: The *LIFETRAC* simulations for on-resonance and detuned WP.

Large number of transverse beam profile measurements along the ring allows us to evaluate the dynamic $\beta_{x,y}^{*+,-}$ values as well as both beam emittances in presence of beam-beam focusing. These measurements by *Lumimetr* software are used routinely to reconstruct luminosity online [19] and serve operator for machine fine-tuning. In Fig. 9 the typical *Lumimetr* predictions (orange dots) together with detectors data (black and red crosses) are shown. Horizontal axis shows the time in seconds.

$$L = 8.477 \times 10^{30} \pm 1.37 \times 10^{30} = 30.52 \text{ nb}^{-1}/\text{hour}$$

Figure 9: Online luminosity monitor @ $E = 800$ MeV.

EXPERIMENTAL RUNS

VEPP-2000 started data-taking with both detectors installed in 2009 [20]. The first runs were dedicated to experiments in the high-energy range [21, 22], while during the last 2012 to 2013 run the scan to the lowest energy limit was done (see Fig. 10). Apart from partial integrability in beam-beam interaction the RBC gives a significant benefit in the Touschek lifetime when compared to traditional flat beams. This results in the ability of VEPP-2000 to operate at an energy as low as 160 MeV — the lowest energy ever obtained in e^+e^- colliders.

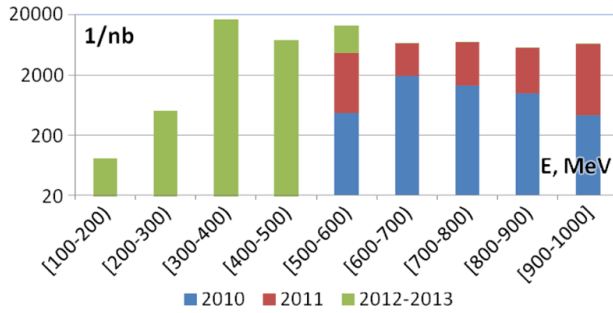


Figure 10: Delivered luminosity in 2010..2013.

The averaged over 10% of best runs luminosity logged by CMD-3 detector during the last three seasons is shown in Fig. 11 with red points. The red lines overestimate the hypothetically achievable peak luminosity with jumps corresponding to possible shortening of FF solenoids by powering only half of coils. The blue dashed line shows the beam-beam limited luminosity for a fixed machine lattice (energy scaling law $L \propto \gamma^4$). It was successfully exceeded due to β^* reduction to 4÷5 cm available at low energies.

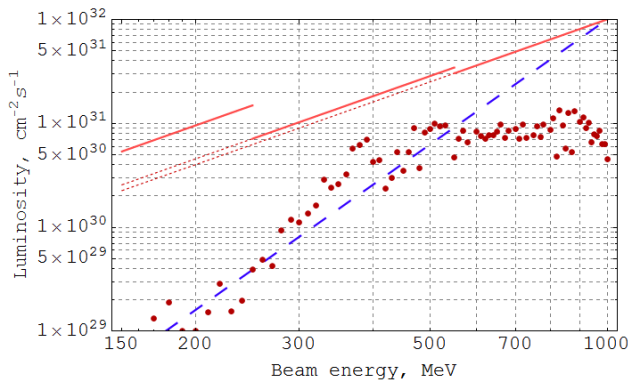


Figure 11: Achieved VEPP-2000 luminosity.

At high energies (> 500 MeV) the luminosity was limited mostly by an insufficient positron production rate (see below). At energies over 800 MeV the necessity of energy ramping in the collider storage ring additionally restricts the luminosity. Only for middle energy range 300÷500 MeV the luminosity is really limited by the beam-beam effects, especially by the flip-flop effect (see below). At the lowest energies the main limiting factors are the small DA, IBS, weak radiation damping, and low beam lifetime as a result.

BEAM-BEAM PARAMETER

We can define the ‘achieved’ beam-beam parameter as:

$$\xi_{\text{lumi}} = \frac{N^- r_e \beta_{\text{nom}}^*}{4\pi\gamma\sigma_{\text{lumi}}^2}, \quad (1)$$

where the beta function is nominal while the beam size is extracted from the fairly measured luminosity.

In Fig. 12 the correlation between achieved and nominal beam-beam parameters is shown for the full data at the

given energy $E = 392.5$ MeV. ‘Nominal’ parameter is defined as (1) but with unperturbed nominal beam size, thus being the measure of beam current. After thorough machine tuning the beam-beam parameter achieves the maximal value of $\xi \sim 0.09$ per one IP during regular work (magenta dots in Fig. 12).

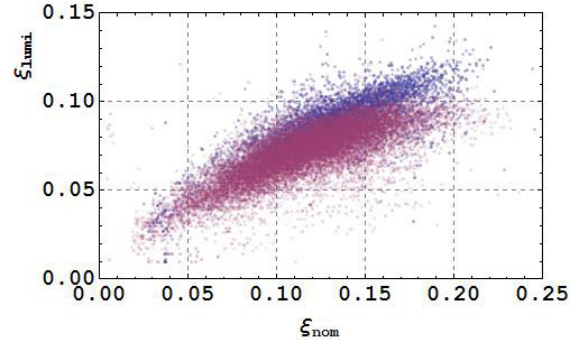
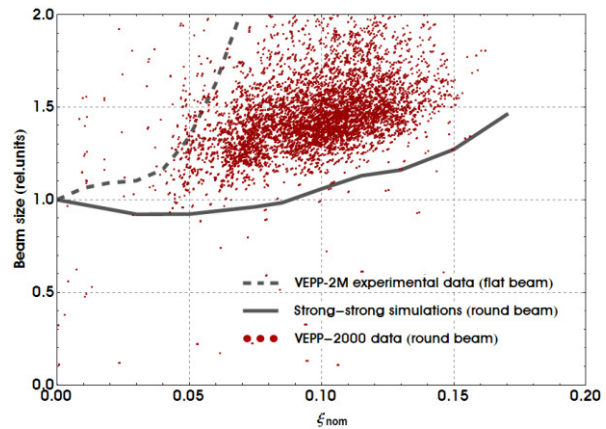


Figure 12: Achieved beam-beam parameter at 392.5 MeV.

Contrary to what the simulations predict (solid line in Fig. 13), the extracted from luminosity beam sizes grow significantly with beam current increase (red dots). However, the emittance grows monotonically, without any blow-up threshold as it happened for flat beam operation at VEPP-2M (dashed line).


 Figure 13: Beam size growth at IP ($E = 537$ MeV).

FLIP-FLOP EFFECT

The beam-beam limit of $\xi_{\text{lumi}} \sim 0.1$ usually corresponds to the onset of a flip-flop effect: the self-consistent situation when one of the beam size is blown-up while another beam size remains almost unperturbed. The simple linear model of flip-flop was discussed earlier [23], with a very high threshold intensity. Observed picture behavior is probably caused by an interplay of beam-beam effects and nonlinear lattice resonances.

In Fig. 14 images from the online control TV camera are presented for the cases of regular beams (a), blown-up electron beam (b) or positron beam (c). The corresponding spectra are shown on the right. One can see in the spectra of a slightly kicked bunch that the shifted tunes (π -mode) jumped to the 1/5 resonance in the case of a flip-flop.

The type of flip-flop effect that has been observed seems to be avoidable by suppressing the resonance driving

terms, as well as by tuning down the working point. Unexpected problems with DA currently prevent us from using the design working point. The acceptable bunch stacking rate and beam lifetime at collision are available only for the betatron tunes of $\{\nu\} \sim 0.13\text{--}0.18$.

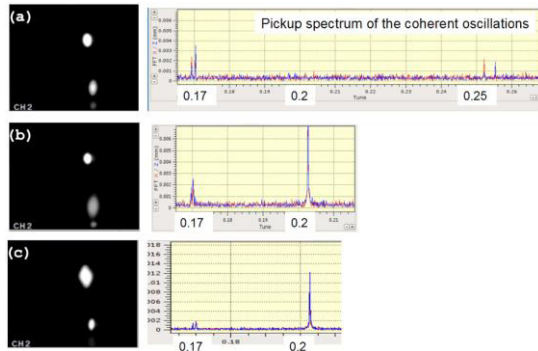


Figure 14: Coherent beam-beam oscillations spectra.

LONG BUNCH

While studying the dependence of beam-beam threshold on bunch length at relatively low energy of 392.5 MeV it was found that the RF voltage decrease from 30 kV to 17 kV gives a significant benefit in the maximal value of ξ (blue dots in Fig. 12) up to $\xi \sim 0.12$ per IP.

The cross-check for beam-beam parameter measurement is the analysis of the coherent beam oscillation spectrum. In Fig. 15 one can find two pairs of σ - and π -modes tunes equal to 0.165 and 0.34, respectively. The total tune shift of $\Delta\nu = 0.175$ corresponds to ξ per one IP equal to:

$$\xi = \frac{\cos(\pi\nu_\sigma) - \cos(\pi\nu_\pi)}{2\pi \sin(\pi\nu_\sigma)} = 0.124. \quad (2)$$

The Yokoya factor here is taken to be equal to 1 due to the fact that oscillations with very small amplitude ($\sim 5 \mu\text{m} = 0.1 \sigma^*$) were excited by a fast kick and the spectrum was investigated for only 8000 turns. During this short time beam distribution is not deformed by an oscillating counter beam and remains Gaussian [24].

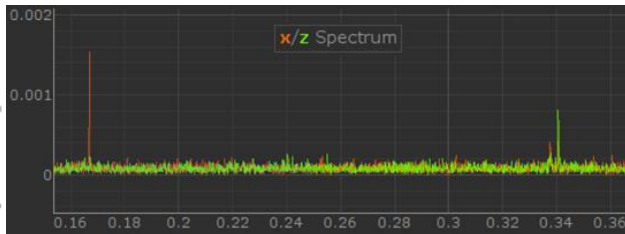


Figure 15: Beam-beam tuneshift @ 392.5 MeV.

The increase of maximal ξ value with lower voltage comes from the bunch lengthening. In our particular case this lengthening is the result of several effects. In addition to regular growth of radiative bunch length two collective effects take place: potential well distortion and microwave instability. The latter one is observed at low energies with a low RF voltage above a certain bunch intensity [14]. In

Fig. 16 the bunch length dependence on beam current is presented for two levels of RF voltage. In Fig. 17 the extracted from horizontal beam size measurements energy spread as a function of intensity is shown. Red points correspond to microwave instability above the threshold.

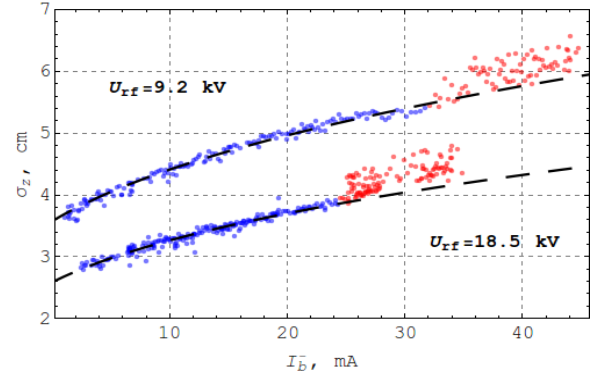


Figure 16: Bunch length as a function of beam current @ $E = 480$ MeV.

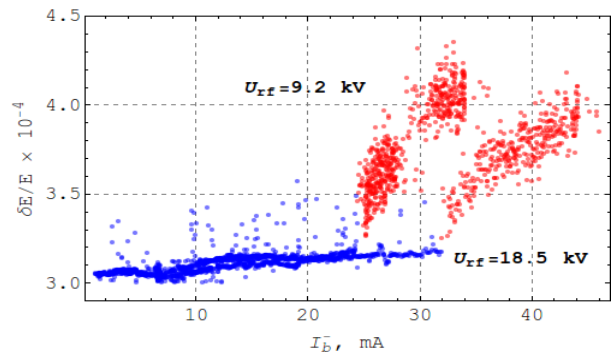


Figure 17: Beam energy spread as a function of beam current @ $E = 480$ MeV.

The observed beam-beam limit enhancement correlated with bunch lengthening firstly believed to be an experimental evidence of predictions [25] of beam-beam interaction mitigation for the bunch slightly longer than β^* due to second integral of motion in addition to the angular momentum. Later it was shown in simulations [26] that finite synchrotron oscillations should prevent full integrability of beam-beam interaction.

Another explanation can come from beam-beam induced resonances suppression due to hour-glass effect [27].

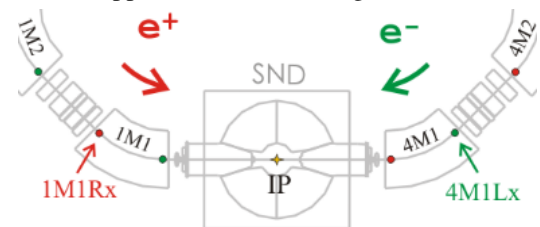


Figure 18: Location of beams size control.

The post-analysis of logged data was done after VEPP-2000 upgrade shutdown had started. At the energy of 392.5 MeV enough data was stored for short (a) and long (b) bunch cases. Only "strong-strong" data was selected, i.e. the beam currents difference does not exceed 10%. In

Fig. 19 the measured horizontal sizes of electron (σ_{4MILx}) and positron (σ_{1MIRx}) beams (see Fig. 18) as a function of beam currents geometric average are shown.

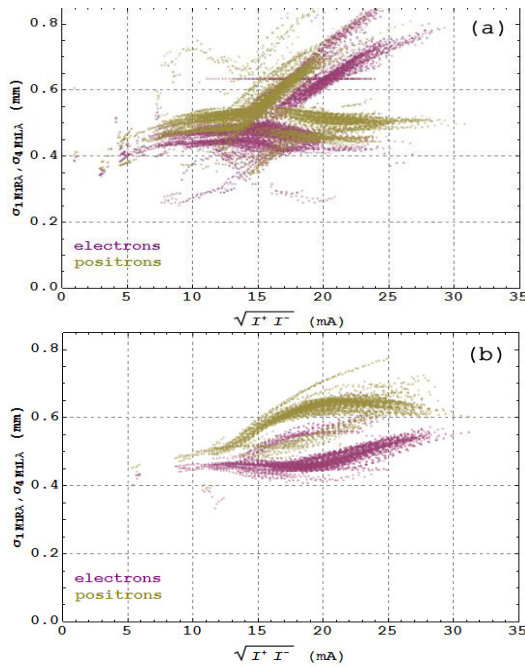


Figure 19: Beam sizes vs. beam current.

These particular sizes (see Fig. 18) are chosen since these observation points are separated from IP by tele-

scopic transformation matrix in horizontal plane and mirror-symmetric to each other. One can see from Fig.19 that in both cases the flip-flop develops (unequal positron and electron beam sizes) for beams intensity higher than 15 mA that corresponds to $\xi_{nom} \sim 0.1$. But the long bunch tends to mitigate this troublesome due to specific luminosity degradation effect for higher intensities.

VEPP-2000 UPGRADE

VEPP-2000 was commissioned and spent three successful runs in 2010-2013 collecting data in the whole energy range of 160÷1000 MeV per beam [28]. In order to achieve the design luminosity the machine was stopped for upgrade of the whole injection chain. Firstly, the complex was linked up via a 250 m beamline K-500 [29] to the new BINP Injection Complex (IC) [30] capable to produce high quality electron and positron beams at energy of 400 MeV (see Fig. 20).

Another VEPP-2000 efficiency limitation came from maximal energy of the booster ring BEP limited at the value of 800 MeV. Even with unlimited e^+/e^- production rate the beam-beam parameter being at the threshold after injection will inevitably decrease after acceleration in the collider ring $\xi \propto 1/\gamma^2$. In addition, the acceleration of colliding beams close to the threshold is very delicate and slow, and leads to a long dead time. As a result, BEP was upgraded to provide top-up injection up to 1 GeV [31]. The transfer channels to VEPP-2000 ring were also reconstructed in order to increase maximal energy.

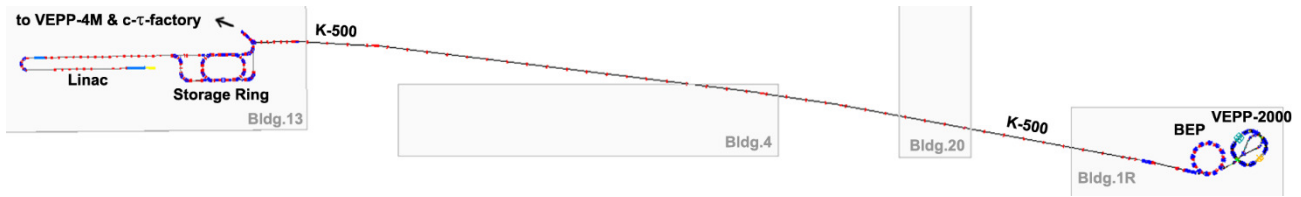


Figure 20: VEPP-2000 linked to the new Injection Complex.

The upgrade was finished in the beginning of 2016. VEPP-2000 injection chain was successfully recommissioned [32]. The achieved positron stacking rate at BEP amounts to $2 \times 10^8 e^+/sec$ that exceeds corresponding value before upgrade in one order of magnitude (see Fig. 21).

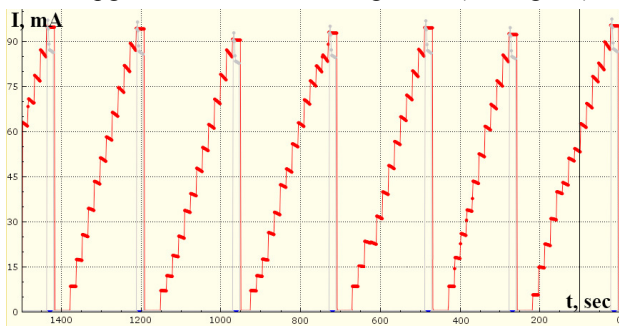


Figure 21: e^+ stacking @ BEP.

Relatively small modifications were done in VEPP-2000 storage ring. Two additional kickers were installed to provide 1 GeV beam injection. All 8 two-sided copper mirrors

used to extract the synchrotron light to CCD cameras were replaced.

In 2016 the collider firstly passed through the beam scrubbing procedure working in so called "warm mode" with switched off SC solenoids. In addition, in this regime two beams e^+/e^- with infinitesimal intensity were obtained to carry out the beam diagnostics alignment and tuning.

During upcoming new run we intend to achieve the target luminosity and start its delivery to detectors with an ultimate goal to deliver at least $1 fb^{-1}$ [33].

CONCLUSION

Round beams give a serious luminosity enhancement. The achieved beam-beam parameter value at middle energies amounts to $\xi \sim 0.1-0.12$. VEPP-2000 was successfully taking data with two detectors across the whole designed energy range of 160–1000 MeV with a luminosity value five times higher than that achieved by its predecessor, VEPP-2M [34]. To reach the target luminosity, injection chain upgrade has been done. Upgraded complex is

now at the finish of the commissioning phase and ready to deliver luminosity at the design level.

ACKNOWLEDGEMENT

We are grateful to M. Achasov, A. Batrakov, E. Bekhtenev, O. Belikov, M. Blinov, D. Burenkov, F. Emanov, K. Gorchakov, G. Karpov, A. Kasaev, A. Kirpotin, I. Korenev, V. Kozak, A. Krasnov, G. Kurkin, P. Logachev, A. Lysenko, S. Motygin, N. Muchnoy, A. Murasev, D. Nikiforov, A. Otboev, V. Prosvetov, A. Romanov, I. Sedlyarov, A. Semenov, A. Senchenko, D. Shatilov, A. Skrinsky, V. Veremeenko, I. Zemlyansky, Yu. Zharinov for continuous support.

REFERENCES

- [1] Yu.M. Shatunov *et al.*, "Project of a New Electron-Positron Collider VEPP-2000", in *Proc. EPAC'00*, Vienna, Austria, 2000, pp. 439-441.
- [2] V.V. Danilov *et al.*, "The Concept of Round Colliding Beams", in *Proc. EPAC'96*, Sitges, Spain, 1996, pp. 1149-1151.
- [3] L.M. Barkov *et al.*, "Phi-Factory Project in Novosibirsk", in *Proc. 14th HEACC'89*, Tsukuba, Japan, 1989, p. 1385.
- [4] K. Ohmi, K. Oide and E.A. Perevedentsev, "The beam-beam limit and the degree of freedom", in *Proc. EPAC'06*, Edinburgh, Scotland, 2006, pp.616-618.
- [5] I. Nesterenko, D. Shatilov and E. Simonov, "Beam-Beam Effects Simulation for VEPP-2M With Flat and Round Beams", in *Proc. PAC'97*, Vancouver, Canada, 1997, p. 1762.
- [6] I.A. Koop, "VEPP-2000 Project", in *Proc. e⁺e⁻ Physics at Intermediate Energies Workshop*, Stanford, 2001, pp. 110-115.
- [7] A.A. Valishev, E.A. Perevedentsev, K. Ohmi "Strong-Strong Simulation of Beam-Beam Interaction for Round Beams", in *Proc. PAC'03*, Portland, USA, 2003, p. 3398.
- [8] E. Young *et al.*, "Collisions of Resonantly Coupled Round Beams at the Cornell Electron-Positron Storage Ring (CESR)", in *Proc. PAC'97*, Vancouver, Canada, 2003, pp. 1542-1544.
- [9] G.M. Tumaikin *et al.*, in *Proc. HEACC'1977*, Serpukhov, USSR, 1977, p.443.
- [10] T.V. Dimova *et al.*, "Recent Results on e⁺e⁻→hadrons Cross Sections from SND and CMD-3 Detectors at VEPP-2000 collider", *Nucl. Part. Phys. Proc.*, vol. 273-275, pp. 1991-1996, 2016.
- [11] S. Henderson *et al.*, "Investigation of the Möbius Accelerator at CESR", in *Proc. PAC'99*, New York, USA, 1999, pp. 410-412.
- [12] Yu.A. Rogovsky *et al.*, "Beam Measurements with Visible Synchrotron Light at VEPP-2000 Collider", in *Proc. DIPAC'11*, Hamburg, Germany, 2011, pp. 140-442.
- [13] Yu.A. Rogovsky *et al.*, "Pickup Beam Measurement System at the VEPP-2000 Collider", in *Proc. RuPAC'10*, Protvino, Russia, 2010, pp. 101-103.
- [14] Yu.A. Rogovsky *et al.*, "Status and Perspectives of the VEPP-2000 Complex", in *Proc. RuPAC'14*, Obninsk, Russia, 2014, pp. 6-10.
- [15] E.V. Abakumova *et al.*, "A system of beam energy measurement based on the Compton backscattered laser photons for the VEPP-2000 electron-positron collider", *Nucl. Instrum. Meth. A*, vol. 744, pp. 35-40, 2014.
- [16] A.L. Romanov *et al.*, "Round Beam Lattice Correction using Response Matrix at VEPP-2000", in *Proc. IPAC'10*, Kyoto, Japan, 2010, pp. 4542-4544.
- [17] I. Koop, E. Perevedentsev, D. Shwartz and A. Valishev, "Correction of the Betatron Coupling and Closed Orbit Distortion at the VEPP-2000 Collider", in *Proc. PAC'01*, Chicago, USA, 2001, pp. 1996-1998.
- [18] D. Shatilov, *Part. Accel.*, vol. 52, p. 65, 1996.
- [19] D. Shwartz *et al.*, "Recent Beam-Beam Effects at VEPP-2000 and VEPP-4M", in *Proc. ICFA Mini-Workshop on Beam-Beam Effects in Hadron Colliders (BB2013)*, Geneva, Switzerland, 2013, CERN-2014-004, pp. 43-49.
- [20] M.N. Achasov *et al.*, "First Experience with SND Calorimeter at VEPP-2000 Collider," *Nucl. Instrum. Meth. A* vol. 598, pp. 31–32, 2009.
- [21] D.N. Shemyakin *et al.*, "Measurement of the e⁺e⁻ → K⁺K⁻π cross section with the CMD-3 detector at the VEPP-2000 collider", *Phys. Let. B*, vol. 756, pp. 153-160, 2016.
- [22] M.N. Achasov *et al.*, "Study of the process e⁺e⁻ → ωηπ⁰ in the energy range $\sqrt{s} < 2$ GeV with the SND detector", *Phys. Rev. D*, 94, 032010, 2016.
- [23] A.V. Otboev and E.A. Perevedentsev. "On self-consistent β-functions of colliding bunches", in *Proc. PAC'1999*, New York, USA, 1999, pp. 1524-1526.
- [24] P.M. Ivanov *et al.*, "Experimental Studies of Beam-Beam Effects at VEPP-2M", in *Proc. Workshop on Beam-Beam Effects in Circular Colliders*, Fermilab, USA, 2001, p. 36.
- [25] V.V. Danilov and E.A. Perevedentsev. "Two Examples of Integrable Systems with Round Colliding Beams", in *Proc. PAC'1997*, Vancouver, Canada, 1997, pp. 1759-1761.
- [26] A. Valishev, S. Nagaitsev, D. Shatilov and V. Danilov, "Beam-Beam Limit in an Integrable System", in *Proc. NaPAC'13*, Pasadena, 2013, pp. 75-77.
- [27] S. Krishnagopal and R. Seeman, "Bunch-length effects in the beam-beam interaction", *Phys. Rev. D*, 41, 2312, 1990.
- [28] A. Romanov *et al.*, "Status of the Electron-Positron Collider VEPP-2000", in *Proc. NaPAC'13*, Pasadena, USA, 2013, pp. 14-18.
- [29] I. Zemlyansky *et al.*, "Electron and Positron Beams Transportation Channels to BINP Colliders", in *Proc. RuPAC'14*, Protvino, Russia, 2014, pp. 462-464.
- [30] A. Starostenko *et al.*, "Status of Injection Complex VEPP-5: Machine Commissioning and First Experience of Positron Storage", in *Proc. IPAC'14*, Dresden, Germany, pp. 538-540.
- [31] D. Shwartz *et al.*, "Booster of Electrons and Positrons (BEP) Upgrade to 1 GeV", in *Proc. IPAC'14*, Dresden, Germany, pp. 102-104.
- [32] D. Berkaev *et al.*, "Commissioning of Upgraded VEPP-2000 Injection Chain", in *Proc. IPAC'16*, Busan, Korea, pp. 3811-3813.
- [33] I. Logashenko *et al.*, "Measurement of hadronic cross-sections with CMD-3 at VEPP-2000", in *Proc. ICHEP'16*, 2016, to be published.
- [34] P.M. Ivanov *et al.*, "Luminosity and the Beam-Beam Effects on the Electron-Positron Storage Ring VEPP-2M with Superconducting Wiggler Magnet", in *Proc. 3rd Advanced ICFA Beam Dynamics Workshop on Beam-Beam Effects in Circular Colliders*, Novosibirsk, USSR, 1989, pp. 26-33.